14

Modeling of Residual Stress

Kumaran Kadirgama[1], Rosli Abu Bakar[1],
Mustafizur Rahman[1] and Bashir Mohamad[2]
[1]*University Malaysia Pahang,*
[2]*University Tenaga Nasional,*
Malaysia

1. Introduction

In many industries, nickel-base alloys represent an important segment of structural materials. Critical components made of these alloys are relied upon to function satisfactorily in corrosive services. The demand for safe, reliable and cost-effective performance requires that these nickel-base alloys provide the anticipated corrosion resistance. Corrosion-resistant high alloy castings are often the subject of major concern because failures of cast components have led to significant downtime costs and operating problems [1]. Over the years, the nickel- chromium-molybdenum / tungsten alloys have proven to be among the most reliable and cost effective materials for aggressive seawater application and excellent resistance to localized corrosive attack (pitting, crevice corrosion).

Among these alloys, Hestelloy C-types (C, C-4, C-276, and C-22) are used to serve the above mentioned purposes. As these alloys are commonly subject to further machining after casting, it becomes very vital to have an idea about the change in properties imparted to the machined surfaces after such cutting operations as end milling. For this reason, finite element methodology is used in this study to determine the machined surface stress characteristics.

In the past decade, finite element method based on the updated-Lagrangian formulation has been developed to analyze metal cutting processes [1-7]. Several special finite element techniques, such as the element separation [1-7], modeling of worn cutting tool geometry [1, 2, 4, 5, 6], mesh rezoning [3, 5], friction modeling [1-7], etc. have been implemented to improve the accuracy and efficiency of the finite element modeling. Detailed work-material modeling, which includes the coupling of temperature, strain-rate, and strain hardening effects, has been applied to model material deformation [3, 5, 6]. An early analytical model for predicting residual stresses was proposed by Okushima and Kakino [8], in which residual stresses were related to the cutting force and temperature distribution during machining. In another analytical model [9] a connection was made between residual stresses and the hardness of the workpiece. Shih and Yang [10] conducted a combined experimental/computational study of the distribution of residual stresses in a machined workpiece. More recently, Liu and Guo [11] used the finite element method to evaluate residual stresses in a workpiece. They also observed that the magnitude of residual stress reduces when a second cut is made on the cut surface. Liu and Barash [12] measured the

residual stress on the workpiece subsurface with consideration of tool flank wear. Their findings indicated that under the condition of a lower cutting speed, the mechanical load had a greater impact on residual stress, while the thermal effect become the major factor effecting residual stress at higher cutting speed. Lee and Shaffer [13] proposed a shear-angle model based on the slip-line field theory, which assumes a rigid-perfectly plastic material behavior and a straight shear plane. Kudo [14] modified the slip-line model by introducing a curved shear plane to account for the controlled contact between the curved chip and straight tool face. Henriksen [15] conducted a series of tests to understand residual stresses in the machined surface of steel and cast iron parts under various cutting conditions. Kono et al. [16] and Tonsoff et al. [17] revealed that residual stresses are dependent on the cutting speed. Matsumoto et al. [18] and Wu and Matsumoto [19] observed that the hardness of the workpiece material has a significant influence on the residual stress field. Konig et al. [20] showed that friction in metal cutting also contributes to the formation of residual stresses.

2. Finite element model

The finite element model is composed of a deformable workpiece and a rigid tool. The tool penetrates through the workpiece at a constant speed and constant feed rate. The model assumes plane-strain condition since generally depth of cut is much greater than feed rate. The finite model used in this study is based on the commercial finite element software. The software, called "Thirdwave AdvantEdge" uses six-noded quadratic triangular elements by default.

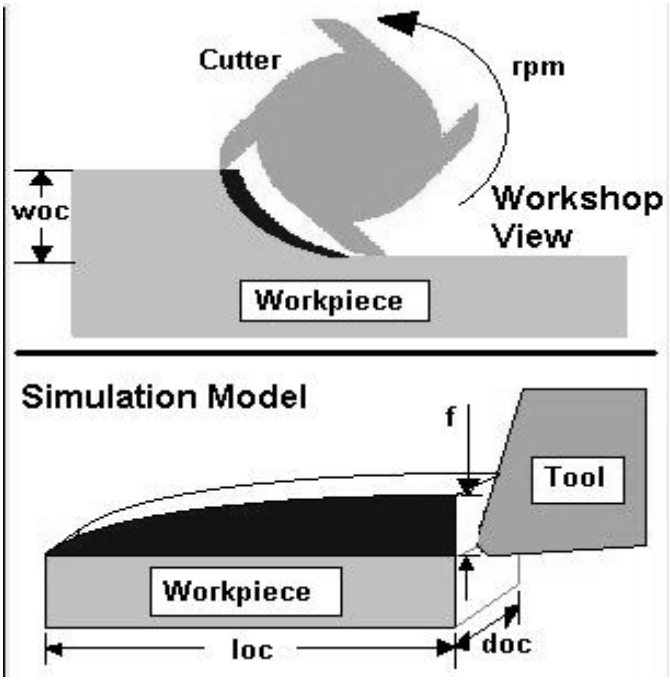

Fig. 1. Thirdwave Advantedge model for milling.

AdvantEdge is an automated program and it is enough to input process parameters to make a two-dimensional simulation of orthogonal cutting operation. The boundary conditions are hidden to the user. Figure 1 shows the Thirdwave AdvantEdge model for milling operation and Figure 2 shows an example of visual simulation of residual stresses induced after milling.

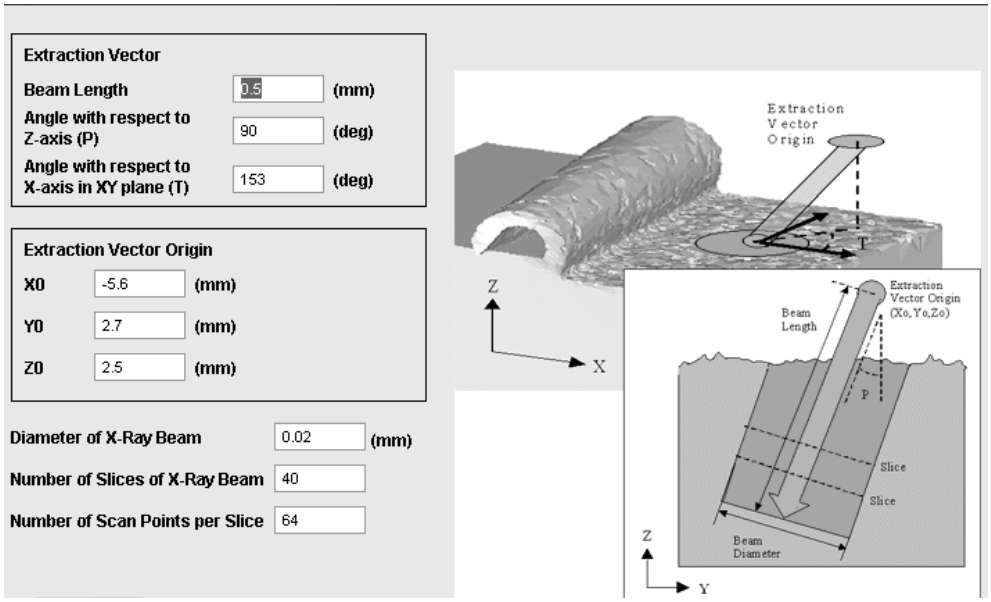

Fig. 2. Thirdwave Advantedge model for residual stress

3. Workpiece and tool material modeling

The workpiece material used for simulation is HASTELLOY C-22HS and the cutting tool is carbide coated with TiALN and 20° rake angle. Every one pass (80mm), the simulation was stopped. AdvantEdge uses an analytical formulation for material modeling. In a typical machining event, in the primary and secondary shear zones very high strain rates are achieved, while the remainder of the workpiece deforms at moderate or low strain rates. In order to account for this, Thirdwave AdvantEdge incorporates a stepwise variation of the rate sensitivity exponent:

$$\bar{\sigma} = \sigma_f\left(\varepsilon^p\right)\cdot\left(1+\frac{\dot{\varepsilon}^p}{\dot{\varepsilon}_o^p}\right)^{1/m_1}, \; if \;\; \dot{\varepsilon} \le \dot{\varepsilon}_t^p \tag{1}$$

where $\bar{\sigma}$ is the effective von Mises stress, σ_f is the flow stress, ε^p is the accumulated plastic strain, $\dot{\varepsilon}_o^p$ is a reference plastic strain rate, m_1 is the strain-rate sensitivity exponents, and $\dot{\varepsilon}_t$ is the threshold strain rate which separates the two regimes. In calculations, a local Newton – Raphson iteration is used to compute $\dot{\varepsilon}_o^p$ according to the low – rate equation, and switches to the high rate equation if the result lies above $\dot{\varepsilon}_t$.

σ_f, which is used in Equation (1) is given as:

$$\sigma_f = \sigma_0 \cdot \psi(T) \cdot \left(1 + \frac{\varepsilon^p}{\varepsilon_0^p}\right)^{1/n} \tag{2}$$

where T is the current temperature, σ_0 is the initial yield stress at the reference temperature T_0, ε_0^p is the reference plastic strain, n is the hardening exponent and $\psi(T)$ is the thermal softening factor. In the present study, it is assumed that the tool is not plastifying. Hence, it is considered as an absolutely rigid body.

4. Results and discussion

Finite Elements simulations were carried out according Table 2. In all simulations, it is made sure that steady- state has been reached and some more data are collected after that time. Therefore, all the results presented in this work were gathered under steady-state condition. From the simulations, variables like stresses, strains, strain rates and temperatures distribution can be obtained. However, all these are very difficult to measure experimentally.

Cutting speed (m/min)	Feedrate (mm/rev)	Axial depth (mm)	Avg. Von Mises stress (Mpa)
140	0.1	2	2100
140	0.2	1	2548
100	0.15	1	1345
100	0.15	2	1548
140	0.15	1.5	2254
100	0.1	1.5	1245
180	0.1	1.5	3987
180	0.15	2	4100
180	0.2	1.5	4488
140	0.2	2	2814
180	0.15	1	4257
140	0.15	1.5	2157
140	0.1	1	1987
100	0.2	1.5	1721
140	0.15	1.5	2347

Table 2: Average value Von mises stress at cutting tool edge

5. Maximum shear stress, stress tensor, Von Mises stress and residual stress

Von Mises stress, σ_V, is used to estimate yield criteria for ductile materials. It is calculated by combining stresses in two or three dimensions, with the result compared to the tensile

strength of the material loaded in one dimension. Von Mises stress is also useful for calculating the fatigue strength [21].

Von Mises stress in three dimensions is expressed as[21]:

$$\sigma_V = \sqrt{\frac{(\sigma_1 - \sigma_2)^2 + (\sigma_2 - \sigma_3)^2 + (\sigma_3 - \sigma_1)^2}{2}} \tag{3}$$

where $\sigma_1, \sigma_2, \sigma_3$ are the principal stresses. In the case of plane stress, σ_3 is zero.

Figure 3 shows the Von mises stress for simulation no.9 (Cutting speed 180 m/min, feedrate 0.15 mm and axial depth 2.0 mm) after 80 mm. Most of the tensile σ_V appear at the cutting tool edge. Based on Von Mises criterion, it states that failure occurs when the energy of distortion reaches the same energy for yield/failure in uniaxial tension. Mathematically, this is expressed as [21],

$$\frac{1}{2}\left[(\sigma_1 - \sigma_2)^2 + (\sigma_2 - \sigma_3)^2 + (\sigma_3 - \sigma_1)^2\right] \leq \sigma_y^2 \tag{4}$$

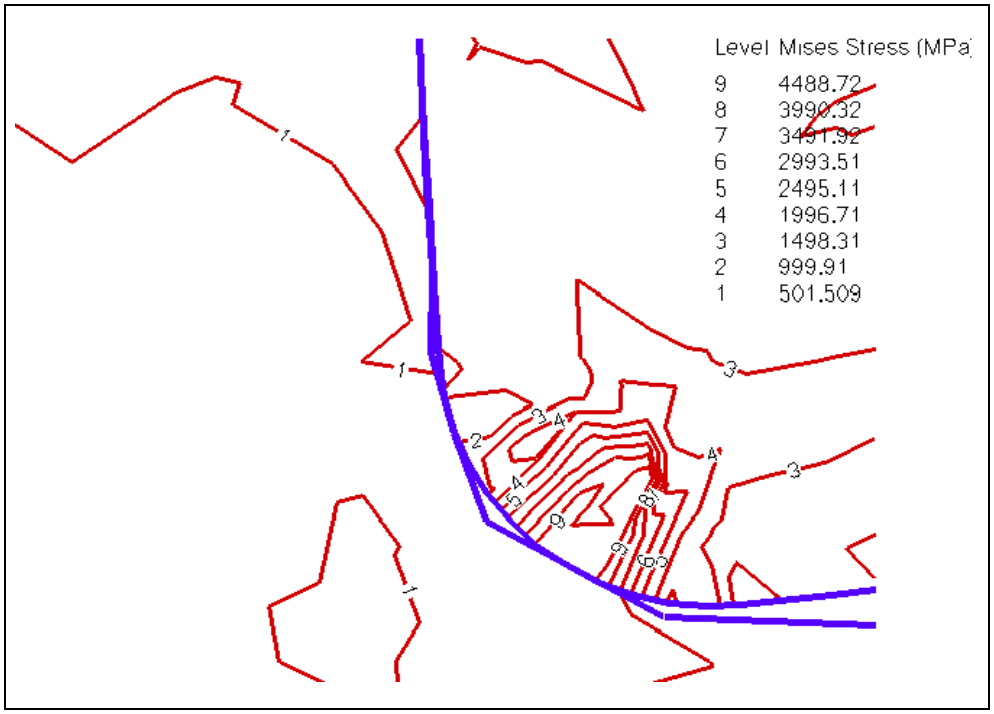

Fig. 3. Von mises stress for simulation no.9.

The yield strength and ultimate tensile strength for the coated carbide cutting tool used in this simulation are 600 MPa and 800 MPa respectively. Then Von Mises stress at at region 9

is 4488 MPa, which is higher than the yield strength and ultimate tensile strength of the coated cutting tool. This strees can cause permanent damage to the cutting tool since this stress is beyond the ultimate tensile strength and yield strength. Cutting speed, feedrate, and axial depth for this simulation is very high and this cause the high stress at the cutting edge, since high cutting speed, feedrate, and axial depth can cause high force in milling [22, 23]. The radial depth for every simulation is 3.5 mm. This factor also contributes to higher stress. At region 1, at the cutting tool and chip contact, the Von mises stress is 501 MPa, where the yield strength and ultimate strength of the workpiece are 359 MPa and 759 MPa. The workpiece start to deform since the stress is above its yield strength.

Figure 4 shows Von Mises stress for simulation no. 3 (Cutting speed 100 m/min, feedrate 0.2 mm/rev, axial depth 1.5 mm). The stress at cutting tool edge (region 5) is 1345 MPa. The Von mises stress is lower compared to that in simulation run no. 9. Even though the stress still higher than yield strength and ultimate tensile strength, but the damage should be not severe compared to that of simulation no.9. At region 3, the stress for the contact point cutting tool and chip is 577 MPa. This value is almost the same as in simulation no.9.

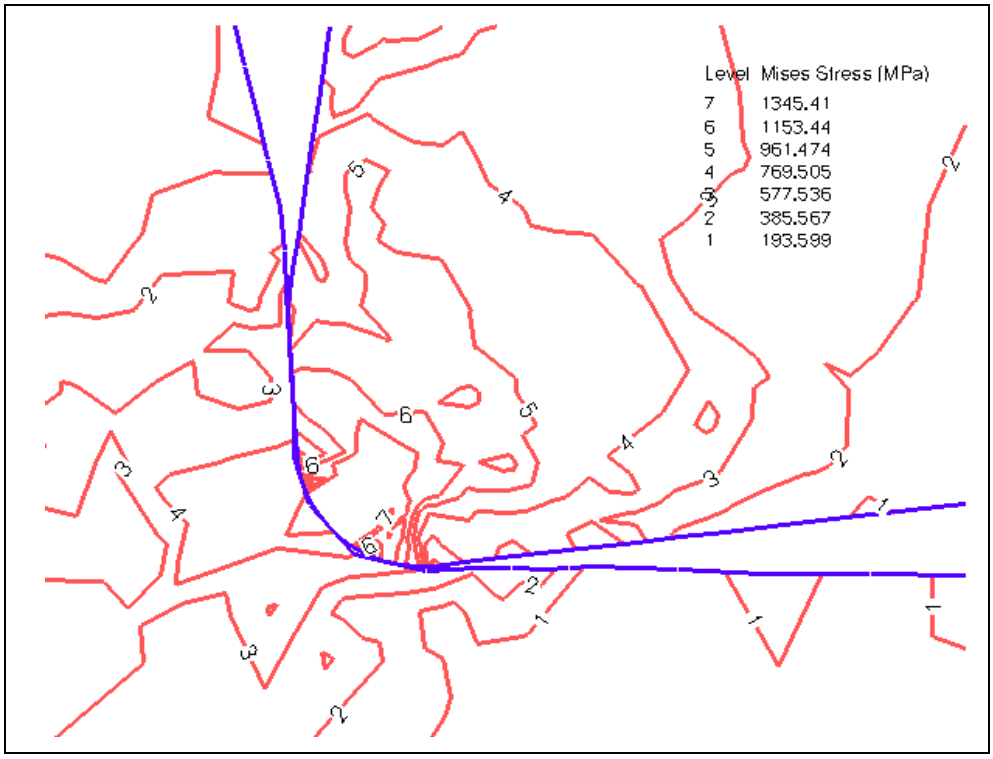

Fig. 4. Von Mises stress for simulation no. 3

From the Von Mises stress distribution as shown in Figure 3 and 4, most of the tensile σ_V locate at the edge of the cutting tool. The stress distribution also show the stress is lower at under the cut surface anFrom the Von Mises stress distribution as shown in Figure 3 and 4,

most of the tensile σ_V locate at the edge of the cutting tool. The stress distribution also show the stress is lower at under the cut surface and increases gradually near the cutting edge. High force is needed at the tool edge for workpiece penetration, and this is indirectly increase the stress at the tool edge. This distribution of the stress is same for both cases. The velocity vectors for simulation no.9 as shown in Figure 5 around the tool tip, clearly show the plastic flow of the material araound the cutting edge. The same trend of flow also was observed by M.S.Gadala et. al. [24]. Figure 6 shows the 3D picture for Von misses stress distribution for simulation no.9.

d increases gradually near the cutting edge. High force is needed at the tool edge for workpiece penetration, and this is indirectly increase the stress at the tool edge. This distribution of the stress is same for both cases. The velocity vectors for simulation no.9 as shown in Figure 5 around the tool tip, clearly show the plastic flow of the material araound the cutting edge. The same trend of flow also was observed by M.S.Gadala et. al. [24]. Figure 6 shows the 3D picture for Von misses stress distribution for simulation no.9.

Table 2 show the average value Von mises stress at cutting tool edge for every simulation that already run. This value will be investigate through statistical method to find the relationship between variables (cutting speed, feedrate and axial depth) with response (Von mises Stress).

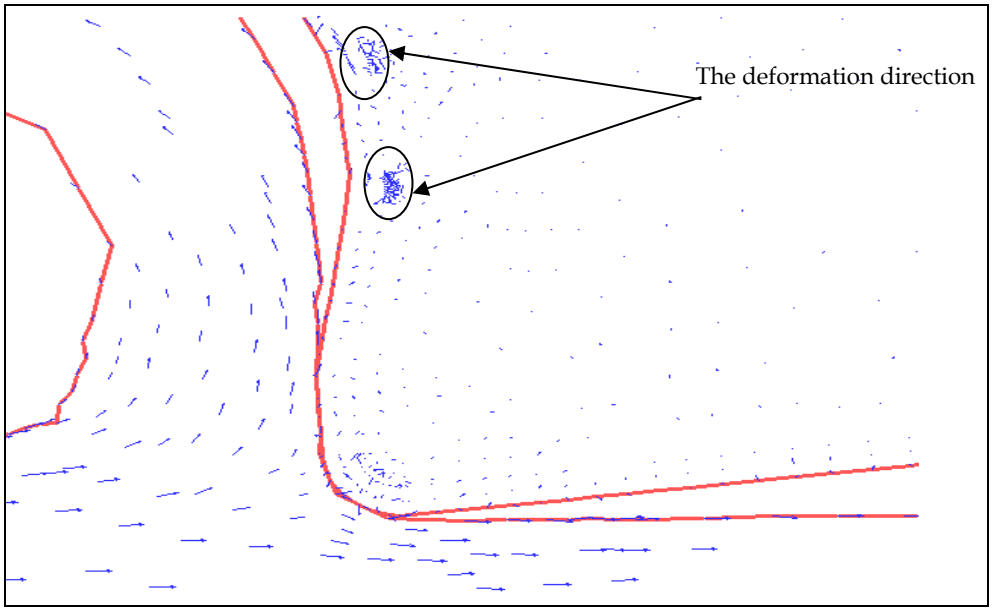

Fig. 5. The velocity vectors for simulation no.9.

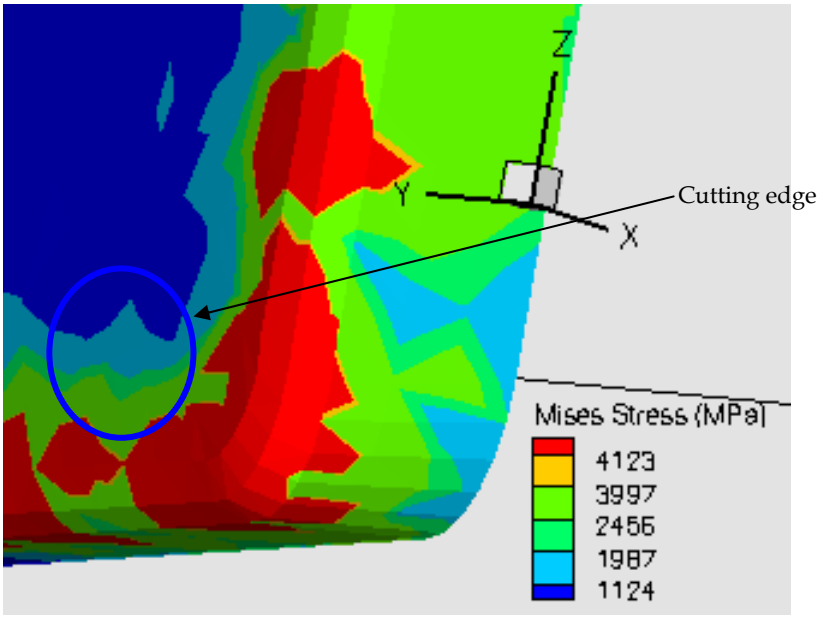

Fig. 6. 3D picture for Von Misses stress distribution for simulation no.9.

6. Conclusion

In the milling operation, cutting speed, feedrate and axial depth play the major role in producing high stresses. The Von Mises stress distribution also show the stress is lower at under the cut surface and increase gradually when come at cutting edge. The highest compressive σ_{xx} appear at the cutting edge. Most of the tensile σ_V appear at the cutting tool edge. The stress distribution also show the stress is lower at under the cut surface and increases gradually near the cutting edge. High force is needed at the tool edge for workpiece penetration, and this is indirectly increase the stress at the tool edge. This distribution of the stress is same for both cases. From the first order model, one can easily notice that the response y (Von Mises stress) is affected significantly by the feed rate followed by axial depth of cut and then by cutting speed. Generally, the increase in feed rate, axial depth and cutting speed will cause Von Mises stress to become larger. The increase in feed rate, axial depth and decrease in cutting speed will cause residual stress to become larger .Response surface method is very useful since with few simulations, a lot of information can be derived such as the relationship between the variables (cutting speed, feedrate and axial depth) with response (Von Mises stress and Residual stress). The combination of numerical analysis and statistical method are very useful to analysis the distribution of stresses in milling.

7. Acknowledgement

The financial support by Malaysian Government through MOSTI and University Tenaga Nasional is grateful acknowledged.

8. References

[1] J. S. Strenkowski and J. T. Carroll, III, A Finite Element Model of Orthogonal Metal Cutting, *ASME 1. Engng Ind.* 107, 345 (1985).

[2] J. S. Strenkowski and G. L. Mitchum, *Proc. North American Manufacturing Conf.,* p. 506 (1987).

[3] A.J.Shih, S. Chandrasekar and H. T. Yang, Fundamental issues in machining, ASME PED-Vol. 43, 11 (1990).

[4] K. Komvopoulos and S. A. Erpenbeek, Finite Element Modelling of orthogonal cutting, *ASME 1. Engng Ind.* 113, 253 (1991).

[5] A.J, Shih and H. T. Yang, Experimental and Finite Element Predictions of Residual Stresses due to Orthogonal Metal Cutting, *Int. I. Numer. Meth. Engng.* 36, 1487 (1993).

[6] A.J. Shih, Finite Element Simulation of Orthogonal Metal Cutting, *ASME 1. Engng Ind.* 117, 84 (1995).

[7] K. Ueda and K. Manabe, Rigid-plastic FEM analysis of three-dimensional deformation fiels in chip formation process *Ann. CIRP* 42, 35 (1993).

[8] K. Okushima, Y. Kakino, The residual stresses produced by metal cutting, Annals of the CIRP 10 (1) (1971) 13–14.

[9] D.W. Wu, Y. Matsumoto, The effect of hardness on residual stresses in orthogonal machining of AISI 4340 steel. Transactions of the ASME, Journal of Engineering for Industry 112 (1990) 245–252.

[10] J. Shih, H.T.Y. Yang, Experimental and finite element predictions of the residual stresses due to orthogonal metal cutting, International Journal for Numerical Methods in Engineering 36 (1993) 1487–1507.

[11] R. Liu, Y.B. Guo, Finite element analysis of the effect of sequential cuts and tool-chip friction on residual stresses in a machined layer, International Journal of Mechanical Sciences 42 (2000) 1069–1086.

[12] C.R. Liu, M.M. Barash, Variables governing patterns of mechanical residual stress in a machined surface. Transactions of the ASME, Journal of Engineering for Industry 104 (1982) 257–264.

[13] E.H. Lee, B.W. Shaffer, The theory of plasticity applied to a problem of machining, Journal of Applied Mechanics 18 (1951) 405–413.

[14] H. Kudo, Some new slip-line solutions for two-dimensional steady state machining, International Journal of Mechanical Science 7 (1965) 43–55.

[15] E.K. Henriksen, Residual stresses in machined surfaces, Transactions ASME Journal of Engineering for Industry 73 (1951) 69–76.

[16] Kono Y, Hara A, Yazu S, Uchida T, Mori Y. Cutting performance of sintered CBN tools, Cutting tool materials. Proceedings of the International Conference, American Society for Metals, Ft. Mitchell, KY, September 15-17, 1980, pp. 218-95.

[17] H.K. Tonshoff, H.G. Wobker, D. Brandt, Tribological aspects of hard turning with ceramic tools, Journal of the Society of Tribologists and Lubrication Engineers 51 (1995) 163–168.

[18] Y. Matsumoto, M.M. Barash, C.R. Liu, Effects of hardness on the surface integrity of AISI 4340 steel. Transactions of the ASME, Journal of Engineering for Industry 108 (1986) 169–175.

[19] D.W. Wu, Y. Matsumoto, The effect of hardness on residual stresses in orthogonal machining of AISI 4340 steel. Transactions of the ASME, Journal of Engineering for Industry 112 (1990) 245–252.

[20] W. Konig, A. Berktold, K.F. Koch, Turning versus grinding—a comparison of surface integrity aspects and attainable accuracy, Annals of the CIRP 42 (1) (1993) 39–43.

[21] J. A. Schey, Introduction to Manufacturing Processes, McGraw Hill,3rd ed, 2000

[22] K.Kadirgama, K.A.Abou-El-Hossein. (2005), 'Force Prediction Model for Milling 618 tool Steel Using Response Surface Methodology', American Journal of Applied Sciences 2(8): 1222-1227, 2005

[23] M.Alauddin,M.A.Mazid, M.A.EL Baradi,M.S.J.Hashmi,"Cutting forces in the end milling of Inconel 718",Journal of Materials Processing Technology",77(1998),pp 153-159

[24] M.Movahhedy, M.S. Gadala, Y. Altintas, "Simulation of the orthogonal metal cutting process using an arbitrary Lagrangian- Eulerian finite –element method", Journal of Materials Processing Technology,103(2000),pp 267-275

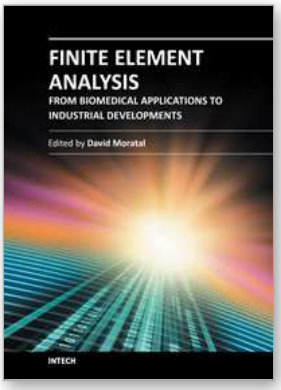

Finite Element Analysis - From Biomedical Applications to Industrial Developments

Edited by Dr. David Moratal

ISBN 978-953-51-0474-2
Hard cover, 496 pages
Publisher InTech
Published online 30, March, 2012
Published in print edition March, 2012

Finite Element Analysis represents a numerical technique for finding approximate solutions to partial differential equations as well as integral equations, permitting the numerical analysis of complex structures based on their material properties. This book presents 20 different chapters in the application of Finite Elements, ranging from Biomedical Engineering to Manufacturing Industry and Industrial Developments. It has been written at a level suitable for use in a graduate course on applications of finite element modelling and analysis (mechanical, civil and biomedical engineering studies, for instance), without excluding its use by researchers or professional engineers interested in the field, seeking to gain a deeper understanding concerning Finite Element Analysis.

INTECH
open science | open minds

InTech Europe
University Campus STeP Ri
Slavka Krautzeka 83/A
51000 Rijeka, Croatia
Phone: +385 (51) 770 447
Fax: +385 (51) 686 166
www.intechopen.com

InTech China
Unit 405, Office Block, Hotel Equatorial Shanghai
No.65, Yan An Road (West), Shanghai, 200040, China
中国上海市延安西路65号上海国际贵都大饭店办公楼405单元
Phone: +86-21-62489820
Fax: +86-21-62489821